# (3+1)D-printed adiabatic 1-to-N couplers

Adrià Grabulosa, Xavier Porte, Johnny Moughames, Daniel Brunner

# (3+1)D-printed adiabatic 1-to-N couplers

Adrià Grabulosa[a], Xavier Porte[a], Johnny Moughames[a], and Daniel Brunner[a]

[a]Institut FEMTO-ST, Université Bourgogne Franche-Comté - CNRS (UMR 6174), 25030 Besançon, France.

## ABSTRACT

Low-loss single-mode optical coupling is a fundamental tool for most photonic networks, in both, classical and quantum settings. Adiabatic coupling can achieve highly efficient and broadband single-mode coupling using tapered waveguides and it is a widespread design in current 2D photonic integrated circuits technology. Optical power transfer between a tapered input and the inversely tapered output waveguides is achieved through evanescent coupling, and the optical mode leaks adiabatically from the input core through the cladding into the output waveguides cores. We have recently shown that for advantageous scaling of photonic networks, unlocking the third dimension for integration is essential. Two-photon polymerization (TPP) is a promising tool allowing dynamic and precise 3D-printing of submicrometric optical components. Here, we leverage rapid fabrication by constructing the entire 3D photonic chip combining one (OPP) and TPP with the (3+1)D flash-TPP lithography configuration, saving up to $\approx$ 90 % of the printing time compared to full TPP-fabrication. This additional photo-polymerization step provides auxiliary matrix stability for complex structures and sufficient refractive index contrast $\Delta n \approx 5 \times 10^{-3}$ between core-cladding waveguides and propagation losses of 1.3 dB/mm for single-mode propagation. Overall, we confront different tapering strategies and reduce total losses below $\sim$ 0.2 dB by tailoring coupling and waveguides geometry. Furthermore, we demonstrate adiabatic broadband functionality from 520 nm to 980 nm and adiabatic couplers with one input and up to 4 outputs. The scalability of output ports here addressed can only be achieved by using the three-spatial dimensions, being such adiabatic implementation impossible in 2D.

**Keywords:** (3+1)D *flash*-printing, two-photon polymerization (TPP), one-photon polymerization (OPP), single-mode low-loss waveguides, broadband adiabatic coupling.

## 1. INTRODUCTION

Recently, we have established the (3+1)D *flash*-TPP as a novel manufacturing methodology that is based on direct-laser writing (DLW) associated with two-photon polymerization (TPP) combined with one-photon polymerization (OPP) for the fabrication of polymer-cladded single-mode 3D optical waveguides 1. Typically, the fabrication of photonic circuits with large volumes, i.e. $mm^3$, using the classical 3D DLW-TPP fabrication results in unfeasible fabrication times 2, 3. To accelerate this process, the (3+1)D *flash*-TPP lithography, first demonstrated with the commercially available IP-S photoresist 4, combines three concepts dedicated to fabricating independently the three essential parts of a photonic circuit: (i) the waveguide cores, (ii) the waveguide cladding and (iii) mechanical support ensuring overall stability. We constrain the high-resolution and slow TPP-trajectories of the waveguide cores, while use fast single-step UV blanket exposure to develop the remaining unstructured cladding volume in one *flash*. Waveguide cores require $\mu$m feature sizes 5, hence a fine resolution in the $(x, y)$-plane, i.e. a small hatching distance $h$, and accurate TPP writing power are crucial to ensure low propagation losses. However, areas acting as mechanical support just need to be mechanically stable and therefore are printed with maximal hatching distances in order to reduce fabrication times. At the same time, we can maximize the vertical distance between consecutive slices, or slicing distance $s$, which does not significantly affect the core-cladding interface roughness and equally accelerates the printing process.

Further author information: (Send correspondence to Adrià Grabulosa)
Adrià Grabulosa: E-mail: adria.grabulosa@femto-st.fr, Telephone: +34 636 64 12 55

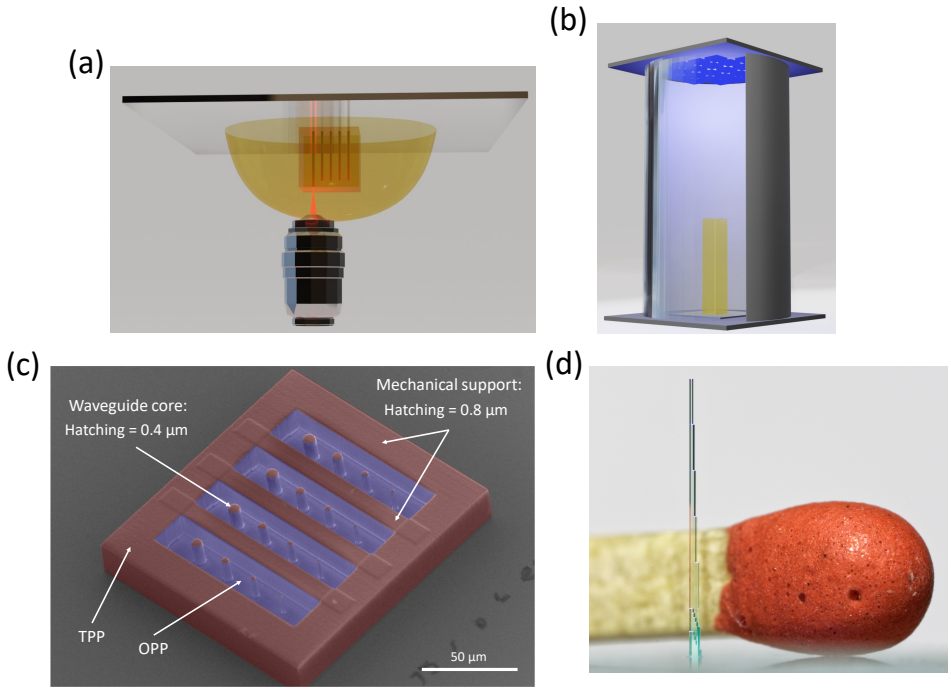


Figure 1. *flash*-TPP for 3D integrated photonics. (a) Illustration of the dip-in process in which the IP-S photoresist is polymerized via DLW-TPP using a fs-laser to fabricate the waveguide cores. (b) A UV light source polymerizes the unexposed regions of the structure, i.e. waveguide cladding. (c) SEM micrograph of a 3D-printed cross-section cutting through a cuboid integrating 16 waveguides with diameters ranging from $d \in \{0.8 : 0.4 : 6.8\}$ $\mu$m. The waveguide cores are printed in high-resolution for maximizing optical performance, while structures only serving mechanical stability are printed with lower spatial resolution. Red colour represents the TPP-printed regions, blue colour represents regions that are polymerized via OPP. (d) Photography of a structure integrating a 6 mm long waveguide size-scaled to a match.

In photonic waveguides, light confinement is caused by total internal reflection at the core-cladding interfaces, being the refractive index of the core ($n_{\text{core}}$) larger than the one of the cladding ($n_{\text{cladding}}$) [6]. To achieve sufficient refractive index contrast $\Delta n = n_{\text{core}} - n_{\text{cladding}}$ for optical guiding, we expose in a single-shot the entire circuit via blanket ultraviolet (UV) irradiation with a controlled exposure dosage $D$ [7, 8]. The working principle of *flash*-TPP is schematically depicted in Fig. 1(a-c). Figure 1(a) depicts the DLW-TPP printing procedure, where the microscope objective is directly immersed into the IP-S photoresist. We use the Nanoscribe GmbH (Photonic Professional GT) system for the TPP-fabrication of waveguide cores and mechanical supports, which is equipped with a femtosecond (fs) laser operating at 780 nm. Then, the unexposed photoresist is removed in a two-step development process using propylene-glycol-methyl-ether-acetate (PGMEA) as a developer for 20 minutes, followed by treatment in isopropyl alcohol (2-propanol) for 3-5 minutes. Finally, we transfer the developed circuit to a UV chamber (Rolence Enterprise Inc., LQ-Box model, 405 nm wavelength, 150 mW/cm$^2$ average light intensity) as shown in Fig. 1(b), by which we control the OPP dosage $D$ determined by the duration of the UV exposure.

The structure in Fig. 1(c) shows a scanning electron microscopy (SEM) micrograph that illustrates the overall (3+1)D *flash*-TPP concept. The 3D photonic circuit is first fabricated in a single 3D DLW-TPP lithography (red region) step, which is followed by OPP via irradiation with the UV light source (blue regions) for several seconds. *flash*-TPP has the advantage of printing 3D microstructures using a dip-in configuration, which allows the fabrication of millimeter-tall yet $\mu$m-diameter waveguides as depicted in Fig. 1(d). Overall, we achieve low 0.26 dB injection losses and propagation losses of 1.36 dB/mm at $\lambda = 660$ nm, while printing vertical single-mode waveguides of 6 mm length that reach refractive index contrast $\Delta n \approx 5 \times 10^{-3}$. The fabrication time is reduced by $\approx 90\%$ compared to only TPP fabrication and the the waveguide's optical performance remains stable during $\sim$600 hours of continuous operation with 0.25 mW injected light [1].

## 2. (3+1)D-PRINTED 1-TO-N BROADBAND ADIABATIC COUPLERS

Here, we use (3+1)D *flash*-TPP lithographic configuration for the fabrication of low-loss single-mode broadband adiabatic couplers with one input and up to 4 outputs. Adiabatic coupling can achieve highly efficient and broadband single-mode coupling using tapered waveguides 9, in which the optical power transfer between a tapered input and inversely tapered output waveguides is achieved through evanescent coupling. Our structures simultaneously split input light to multiple adiabatic tapered output ports. However, the majority of demonstrations and studies before consider the 2D case of 1 to 1 waveguide adiabatic tapered coupling 10, 11. Our *flash*-TPP fabricated adiabatic couplers have ultra-low global losses of $\sim 0.2$ dB, while the losses remain $< 2$ dB for a remarkable range of $\Delta\lambda \sim 500$ nm.

For the adiabatic couplers here presented, we tapered the waveguide cores comparing two different strategies as shown in Fig. 2 (a), where the left (right) panel shows conical (truncated rod) geometries, respectively. In both, the waveguide cross-section continuously changes along the propagation direction from an input diameter $d$ through a taper-length $l_\mathrm{t}$, which is intrinsically linked to the beating length $z_\mathrm{b}$ 6. In the conical geometry, the waveguide cross-section shrinks equally in both, $(x, y)$ directions. However, for the truncated rod geometry, one direction is fixed to $d$ while the other linearly shrinks along the taper positions within $l_\mathrm{t}$. This unique spatially-invariant aspect of the truncated rod design offers coupling parallel to the splitting direction and increases the interface-area for effective signal transfer. We inversely tapered input and output waveguides with equal taper-rate and therefore identical symmetry in order to match their effective modal index. We added a straight section $l = 30$ $\mu$m to all output ports in order to minimize the cross-talk outside the tapered regions, and we separate neighboring waveguides by a gap $g$ between the input and output waveguides.

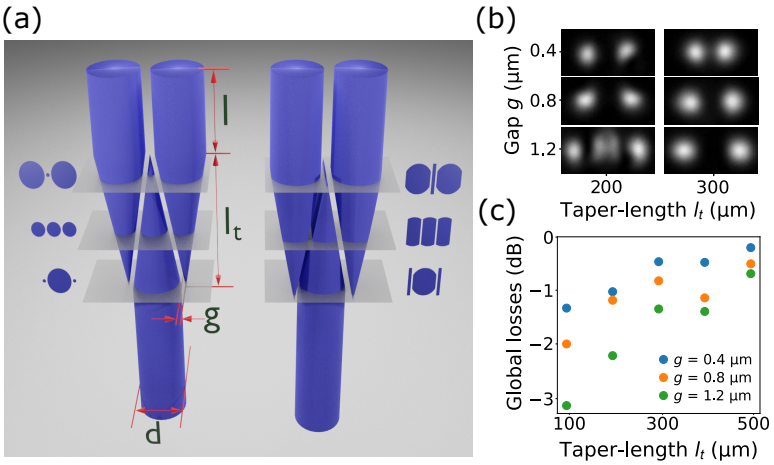


Figure 2. Design and global losses of 1 to 2 adiabatic couplers. (a) Design of the conical (left) and truncated rod (right) geometries of (3+1)D *flash*-TPP printed 1 to 2 adiabatic splitters. (b) Output intensity profiles of the 1 to 2 adiabatic couplers with truncated rod geometry for taper-length $l_\mathrm{t} = 200$ $\mu$m (left) and $l_\mathrm{t} = 300$ $\mu$m (right) for gaps $g \in \{0.4,\ 0.8,\ 1.2\}$ $\mu$m (top to bottom). (c) Global losses of 1 to 2 couplers with truncated rod geometry for gaps $g$ and taper-lengths $l_\mathrm{t} \in \{100 : 100 : 500\}$ $\mu$m

We perform ultra-rapid fabrication by constructing the entire 3D photonic chip combining one- (OPP) and two-photon polymerization (TPP) with the (3+1)D *flash*-TPP lithography, saving up to $\approx 90$ % of fabrication time 1. The waveguide cores are embedded in a 3D cuboid and printed in a single-step via DLW-TPP using the commercial 3D direct-laser writing Nanoscribe GmbH (Photonics Professional GT) system. The liquid negative-tone IP-S photoresist is polymerized via TPP with a femtosecond (fs) laser operating at 780 nm that is tightly focused into the immersion medium thought a high-numerical aperture (NA = 0.8) 25X objective lens forming writing voxels within the focal point. The fs-laser beam is rapidly moved by galvanometer mirrors in the lateral directions and then translated along the vertical positions for a precise layer-by-layer additive manufacturing. The waveguides cores are printed with an optimal laser power (LP = 15 mW) and high-resolution ($h = 0.4$ $\mu$m) to ensure smooth surfaces and low propagation losses, while mechanical supports, i.e. the cuboid-surface, are

printed with larger hatching distance ($h = 0.8$ $\mu$m). The slicing distance is maximized to $s = 1$ $\mu$m. After fully-TPP of the IP-S photoresist ($n = 1.510$), the unexposed photoresist is removed following a standard two-step development process. Finally, the entire 3D photonic circuit is treated via OPP with a UV exposure dose of D = 3000 mJ/cm$^2$ (see Fig. 1(a-c)). This additional photopolymerization step provides auxiliary matrix stability for complex structures and sufficient refractive index constrats $\Delta n \approx 5 \times 10^{-3}$ between core-cladding waveguides and hence optical confinement for single.mode propagation 1.

We evaluate the global losses (injection, coupling and propagation) for gaps $g \in \{0.4,\ 0.8,\ 1.2\}$ $\mu$m between input and output 1 to 2 adiabatic splitters. Noteworthy, we present here the extensive results for the truncated rod geometry only as we found to have on average $\sim 3$ times less global losses. The waveguide cores are linearly tapered from an input-taper diameter $d = 3.3$ $\mu$m. We tune the taper-length $l_t$ from 100 to 500 $\mu$m and find adiabatic conditions for a taper-length $l_t > 200$ $\mu$m, as shown in the output intensity profiles of Fig. 2(b). It is clear that for $l_t = 200$ $\mu$m (left) the outputs profiles for $g = 0.4$ $\mu$m (top) and $g = 0.8$ $\mu$m (middle) are not single-mode, and for $g = 1.2$ $\mu$m (bottom) are not completely separated. However, we obtain full splitting of optical single-modes for $l_t = 300$ $\mu$m (right) for all $g$. Consequently, the adiabatic criterion of the 1 to 2 couplers is fulfilled for a taper-length $l_t > 200$ $\mu$m, which agrees with the theoretical prediction for adiabaticity $l_t > z_b = \lambda/\Delta n \approx 132$ $\mu$m, where $\lambda = 660$ nm is the wavelength in the vacuum. Finally, Fig. 2(c) shows the global losses of the 1 to 2 adiabatic couplers with truncated rod geometry for different gaps $g$. Global losses are minimized to $\sim 0.2$ dB and the output intensities only differ by $\sim 3.4$ % between the two output ports for $l_t = 500$ $\mu$m and $g = 0.4$ $\mu$m. The experimentally measured high optical power transfer certifies the adiabatic signature of our splitters, which is a hallmark of evanescent transition and further demonstrates the high-quality of our adiabatic couplers with truncated rod geometry.

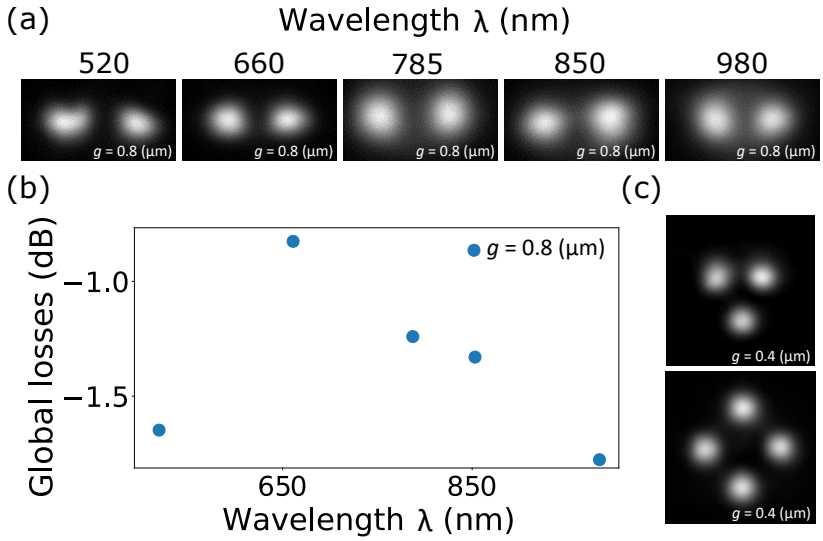


Figure 3. Broadband functionality and 1 to 3 and 4 adiabatic couplers. (a) Global losses versus injection light wavelength $\lambda$ of the 1 to 2 adiabatic couplers with $l_t = 500$ $\mu$m and $g = 0.8$ $\mu$m. (b) Output intensity profiles from (a) over $\Delta\lambda \sim 500$ nm. (c) Output intensity profiles of the 1 to 3 (top) and 1 to 4 (bottom) adiabatic couplers with $l_t = 500$ $\mu$m and $g = 0.4$ $\mu$m.

Generally, adiabatic transfer offers wavelength-independent splitting of optical signals. We inject light ranging from $\lambda = 520$ nm to $\lambda = 980$ nm to our 1 to 2 adiabatic couplers with $l_t = 500$ $\mu$m, and Fig. 3(a) shows the output intensity profiles of the couplers across this entire range of wavelengths. For $\lambda \geq 660$ nm, the lower confinement of the fundamental mode leads to a signal spreading towards the cladding, and therefore a larger gap $g = 0.8$ $\mu$m is required for its complete adiabatic transfer. However, for $\lambda = 520$ nm, higher-order propagation modes are excited and launched into the waveguides. Finally, Fig. 3(b) depicts global losses that remain below $\sim$ 2dB for the 1 to 2 adiabatic couplers over the $\Delta\lambda \sim 500$ nm range here evaluated.

In a last investigation, we fabricate 1 to 3 and 4 adiabatic couplers, where the cross-sections of the waveguides are triangular and quadrangular pyramids for the 1 to 3 and 1 to 4 adiabatic couplers, respectively. Figure 3(c)

shows the single-mode splitting outputs for 1 to 3 (top) and 1 to 4 (bottom) adiabatic couplers with $l_t = 500$ $\mu$m and $g = 0.4$ $\mu$m. Total losses are only $\sim 0.7$ dB and the intensity difference between output ports is $\sim 4.6$ % for 1 to 3 and $\sim 6.1$ % for 1 to 4 adiabatic couplers, respectively.

Overall, we use the novel (3+1)D *flash*-TPP lithography configuration for the manufacturing of single-mode low-loss broadband 3D adiabatic couplers with one input and up to 4 output ports. After comparing different tapering geometries for adiabatic transfer, the global losses are reduced to $\sim 0.2$ dB and the adiabatic broadband functionality with losses $< 2$ dB over $\Delta\lambda \sim 500$ nm is demonstrated. The scalability of output ports here addressed can only be achieved by using the three spatial dimensions, hence unlocking the third dimension results crucial for such implementation 12,13. This demonstrates our *flash*-TPP printing technology as a powerful tool for complex and CMOS compatible 3D integrated photonic circuits.

## REFERENCES


[1] Grabulosa, A., Moughames, J., Porte, X., and Brunner, D., "Combining one and two photon polymerization for accelerated high performance (3 + 1)d photonic integration," *Nanophotonics* **11**(8), 1591–1601 (2022).

[2] Lindenmann, N., Balthasar, G., Hillerkuss, D., Schmogrow, R., Jordan, M., Leuthold, J., Freude, W., and Koos, C., "Photonic wire bonding: a novel concept for chip-scale interconnects," *Optics Express* **20**, 17667 (2012).

[3] Pyo, J., Kim, J. T., Lee, J., Yoo, J., and Je, J. H., "3d printed nanophotonic waveguides," *Advanced Optical Materials* **4**(8), 1190–1195 (2016).

[4] Schmid, M., Ludescher, D., and Giessen, H., "Optical properties of photoresists for femtosecond 3d printing: refractive index, extinction, luminescence-dose dependence, aging, heat treatment and comparison between 1-photon and 2-photon exposure," *Optical Materials Express* **9**, 4564 (12 2019).

[5] Selvaraja, S. K. and Sethi, P., "Review on optical waveguides," *Emerging Waveguide Technology* **2** (2018).

[6] Snyder, A. W. and Dove, J. D., [*Optical Waveguide Theory*], Chapman and Hall (1983).

[7] Eschenbaum, C., Großmann, D., Dopf, K., Kettlitz, S., Bocksrocker, T., Valouch, S., and Lemmer, U., "Hybrid lithography: Combining UV-exposure and two photon direct laser writing," *Optics Express* **21**(24), 29921 (2013).

[8] Lim, M. P., Guo, X., Grunblatt, E. L., Clifton, G. M., Gonzalez, A. N., and LaFratta, C. N., "Augmenting mask-based lithography with direct laser writing to increase resolution and speed," *Optics Express* **26**(6), 7085 (2018).

[9] Son, G., Han, S., Park, J., Kwon, K., and Yu, K., "High-efficiency broadband light coupling between optical fibers and photonic integrated circuits," *Nanophotonics* **7**, 1845–1864 (oct 2018).

[10] Marchetti, R., Lacava, C., Carroll, L., Gradkowski, K., and Minzioni, P., "Coupling strategies for silicon photonics integrated chips," *Photon. Res.* **7**, 201–239 (Feb 2019).

[11] Tsuchizawa, T., Yamada, K., Fukuda, H., Watanabe, T., ichi Takahashi, J., Takahashi, M., Shoji, T., Tamechika, E., Itabashi, S., and Morita, H., "Microphotonics devices based on silicon microfabrication technology," *IEEE Journal of Selected Topics in Quantum Electronics* **11**(1), 232–240 (2005).

[12] Porte, X., Dinc, N. U., Moughames, J., Panusa, G., Juliano, C., Kadic, M., Moser, C., Brunner, D., and Psaltis, D., "Direct (3+1)D laser writing of graded-index optical elements," *Optica* **8**, 1281 (oct 2021).

[13] Moughames, J., Porte, X., Thiel, M., Ulliac, G., Larger, L., Jacquot, M., Kadic, M., and Brunner, D., "Three-dimensional waveguide interconnects for scalable integration of photonic neural networks," *Optica* **7**, 640 (jun 2020).